PAPER

Check for updates

Uranyl fluorescence in acidic solution: quenching effects by tetramethylammonium (TMA⁺)†

Thomas D. Persinger, [iD] *[a] Michael C. Heaven [iD] [b] and Richard E. Wilson [iD] [a]

The quenching of uranyl luminescence by various cation species was studied in aqueous media at low pH. Solutions with different nitrate salts, held at constant uranyl nitrate, nitric acid, and ion concentration, were tested to examine the quenching effects of the cations from the nitrate salts. Alkali metal (Li⁺, Na⁺, Rb⁺) and quaternary ammonium cations (NH₄⁺), $(CH_3)_4N^+$ (TMA⁺), $(C_2H_5)_4N^+$ (TEA⁺) were investigated. Solutions containing TMA⁺ reduced the lifetime of uranyl fluorescence significantly more than the other cations. Uranyl emission spectra also showed that TMA⁺ increased the complex formation between uranyl and nitrate ions. Fluorescence decay lifetime measurements for most solutions yielded values between 1.4–1.9 μs at 20 °C, while 1.8 M TMA⁺ reduced the lifetime of uranyl fluorescence to 0.6 μs. Decay rate *versus* concentration data (Stern–Volmer plots) indicated a dynamic quenching process with increasing fluorescence decay rates at higher cation concentrations for Li⁺, TMA⁺, and TEA⁺. The temperature dependencies of the decay rates and the kinetics in D_2O were also examined.

1. Introduction

Solution chemistry involving the uranyl ion (UO_2^{2+}) and its interactions with the surrounding molecules in aqueous environments is important for research in nuclear waste management, environmental remediation, and heavy element separations.[1] Speciation effects on UO_2^{2+} in solution is a multi-faceted problem that is still not completely understood. The complexation of UO_2^{2+} in nitric acid solution has been explored,[2,3] where the low-pH environment results in the formation of UO_2^{2+}–nitrate complexes. However, the equilibrium of these complexes in solution can be impacted by many factors. The introduction of additional molecules, both as electrolytes and coordinating ligands in solution leads to a variety of physical and chemical interactions with UO_2^{2+} that are difficult to predict. Photoexcitation of UO_2^{2+} populates a highly reactive excited state where it behaves as a strong oxidizer,[4] leading to a variety of interactions with nearby molecules and providing alternative pathways for electronic relaxation. The quenching of UO_2^{2+} luminescence by some ions such as carbonate and chloride is efficient enough that even at low concentrations, they can make it difficult to determine uranyl concentrations in solution. Transient absorption spectroscopy (TAS) was used to understand the quenching mechanism of chloride and bromide. It was found that the halogen anions interacted with UO_2^{2+}

through the equatorial plane and the uranyl solvent shell influenced the anion's ability to quench the luminescence.[5] To effectively use uranyl luminescence for monitoring processes we must understand the mechanisms by which UO_2^{2+} interacts with other solute molecules, particularly cations that may facilitate the formation of ion-pairs or other ion–ion interactions.

Tetramethylammonium (TMA⁺) has been shown to uniquely modify UO_2^{2+} speciation in solution, presumably through the formation of ion-pair complexes. Hydrolysis experiments of UO_2^{2+} can be challenging to perform because, under alkaline conditions, insoluble uranyl hydroxide salts begin to form. However, TMA⁺ was found to be an effective supporting electrolyte in solution as its presence inhibited the formation of insoluble uranyl salts.[6] Clark *et al.* used this interaction between UO_2^{2+} and TMA⁺ to spectroscopically characterize larger uranyl hydroxide species $(UO_2(OH)_n^{2-n}$ (n = 4, 5)).[7] They also discovered that this behavior was unique to TMA⁺ and that larger and smaller ammonium ions did not prevent uranyl salts from precipitating out of the solution. It appears that TMA⁺ participates in some interaction with UO_2^{2+} in solution, but the details are not yet known. The interaction with TMA⁺ has not been investigated in a low-pH solution, where the uranyl does not form hydroxides. Studies at low pH may provide new insights concerning the nature of the UO_2^{2+}/TMA⁺ interaction and the possibility of ion association.

Time-resolved and steady-state fluorescence spectroscopy are powerful techniques that are used to investigate the interactions between UO_2^{2+} and the surrounding molecules in solution, facilitating the measurement of their thermodynamic formation constants and highlighting the impact of the local

[a] *Chemical Sciences and Engineering Division, Argonne National Laboratory, Lemont, Illinois 60439, USA. E-mail: tpersinger@anl.gov*

[b] *Emory University, Atlanta, Georgia 30322, USA*

chemical environment on the UO_2^{2+} luminescence spectrum. Extensive studies have shown that UO_2^{2+} is subject to many types of quenching interactions, including electron transfer,[5,8,9] hydrogen abstraction,[10,11] self-quenching,[12] and exciplex formation.[2,13] These processes result in faster fluorescence decay rates for the excited UO_2^{2+} and studying how temperature and solute concentrations affect the rates can provide insight into the mechanism by which the UO_2^{2+} fluorescence is being quenched.[14] In the present study, we explore the fluorescence quenching abilities of alkali metal and quaternary ammonium cations. Measurements were taken over a range of temperatures. Solvent effects were probed by comparing results obtained in H_2O and D_2O. Concentration dependences were determined to differentiate between static and dynamic quenching processes.

2. Experimental methods

2.1. Sample preparation

The $UO_2(NO_3)_2 \cdot 6H_2O$ used for these experiments was obtained from an Argonne 0.2 M stock solution prepared in 20 mM nitric acid. The $NaNO_3$, $LiNO_3$, $RbNO_3$, $(CH_3)_4NNO_3$, and $(C_2H_5)_4$-NNO_3 salts (Fisher Chemicals), and the deuterated solutions D_2O, DNO_3 and $(CD_3)_4NNO_3$ (Sigma Aldrich) were used to make 2 M stock solutions by dissolving the appropriate mass of nitrate salt in a 20 mM nitric acid solution to keep a consistent acid concentration. Varied salt concentrations for each sample were made by mixing the appropriate volumes of these stock solutions into 2 mL vials. For storage, the vials were sealed using parafilm. For optical measurements the samples were transferred *via* pipette into quartz fluorescence cuvettes.
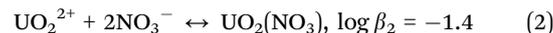
2.2. Instrumentation

All fluorescence experiments were carried out using an FLS1000 photoluminescence spectrometer (Edinburgh Instruments), equipped with an Opolette 355 (Opotek) OPO tunable pulsed laser source. Samples were placed inside fluorescence cuvettes

and a variable-temperature stage was used to study fluorescence from 5–40 °C. Quenching behavior in the solution was investigated *via* lifetime measurements of uranyl transitions using the pulsed (10 ns) OPO source. Continuous stirring of the solution was used to avoid the effects of local heating caused by the absorption of the excitation laser pulses. The fluorescence was dispersed by a monochromator and the wavelength-selected light was collected using a photomultiplier tube (Hamamatsu, PMT-900) with a multichannel scaling (MCS) photon counting method. The signals were processed and plotted using the in-house Edinburgh program (Fluoracle). A Xenon lamp source was used in conjunction with excitation and emission monochromators to collect the excitation and emission spectra of the uranyl species.

3. Results and analyses

3.1. Steady-state emission

The quenching properties of alkali metal and quaternary ammonium cations were explored using time-resolved laser fluorescence spectroscopy (TRLFS) and steady-state emission spectroscopy. At a concentration of 20 mM $[UO_2^{2+}]$ and 20 mM $[HNO_3]$ (pH = 1.7), hydroxide complexation with uranyl was avoided. The primary complexation with the uranyl aqua ion in solution was with the nitrate ion (NO_3^-), which formed uranyl nitrate complexes ($UO_2(NO_3)_n^{2-n}$) described by the following equations of equilibrium,[3]

$$UO_2^{2+} + NO_3^- \leftrightarrow UO_2NO_3^+, \log \beta_1 = -0.45 \quad (1)$$

$$UO_2^{2+} + 2NO_3^- \leftrightarrow UO_2(NO_3), \log \beta_2 = -1.4 \quad (2)$$

where β_1 and β_2 are equilibrium constants for chemical eqn (1) and (2) respectively and describe the stability of the complex formation in solution.

The samples prepared in this study contained nitrate salt concentrations between 0–1.8 M. As nitrate concentration in the solution increased, the emission spectra broadened due to
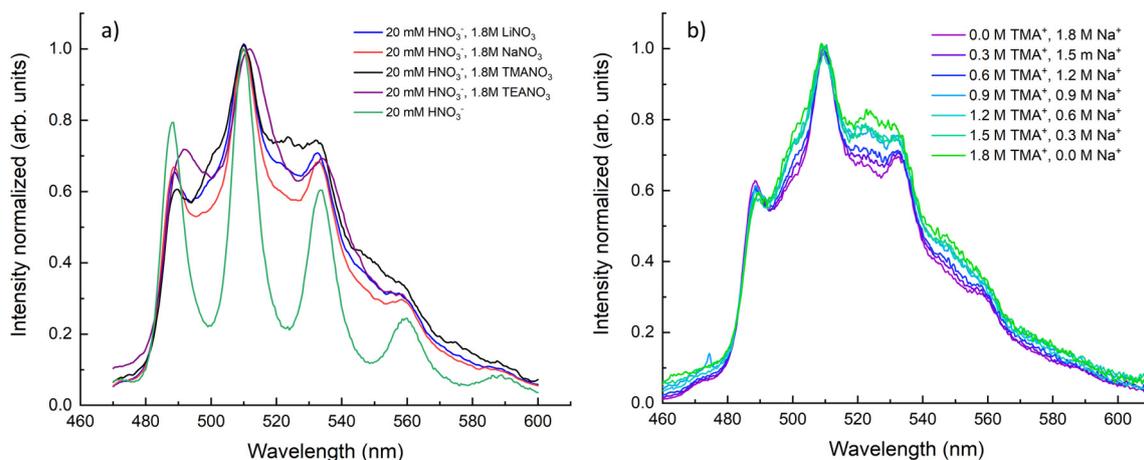

Fig. 1 Steady-state emission spectra of uranyl from 460–600 nm. (a) The emission from solutions containing Li+, Na+, TMA+, and TEA+ nitrate salts are compared to uranyl nitrate in nitric acid. (b) Change in emission bands as $NaNO_3$ is replaced with $TMANO_3$. Excitation wavelength was 394 nm for all samples.

This journal is © the Owner Societies 2025

Phys. Chem. Chem. Phys., 2025, **27**, 10166–10173 | **10167**

increasing uranyl nitrate complexation.[3,15,16] The steady-state emission spectra in Fig. 1 show the UO_2^{2+} fluorescence from the lowest excited electronic state $T_1(^3\Delta) \rightarrow S_0(^1\Sigma^+)$. An excitation energy of 394 nm was used, which promoted UO_2^{2+} into the $T_2(^3\Phi)$ excited electronic states before quickly undergoing non-radiative decay into the lower $T_1(^3\Delta)$ state.[9,17,18] The emission spectra show the ground state symmetric stretch vibrational progression. The spectra in Fig. 1a (left) show that the addition of all nitrate salts resulted in the broadening of emission bands due to complexation with nitrate. Uranyl nitrate complexation red-shifted the emission spectra, and the presence of multiple uranyl species caused the observed spectral broadening. Fig. 1b shows that the cations did not have a uniform effect on uranyl complexation. The replacement of Na^+ with TMA^+ resulted in greater complexation, which could be explained by TMA^+ pushing the equilibrium of eqn (1) and (2) to the right. This shift in equilibrium could be due to ion interactions between UO_2^{2+} and TMA^+.

3.2. Time-resolved laser fluorescence spectroscopy (TRLFS)

For the measurement conditions used in the present study, it is pertinent to consider the speciation of UO_2^{2+} in the presence of relatively high nitrate concentrations (up to 1.8 M). Moulin *et al.*[3] analyzed uranyl emission spectra taken in low pH nitrate solutions to probe the speciation. For 1.8 M NO_3^-, their data show that the speciation would be 50% UO_2^{2+}, 40% $UO_2^+NO_3$, and 10% $UO_2(NO_3)_2$ (see Fig. 2 of ref. 3).

In the TRLFS experiments the control conditions (aqueous solution with 20 mM $[UO_2^{2+}]$ and 20 mM $[HNO_3]$) yielded a fluorescence lifetime of 1.9 μs at 20 °C. The addition of 1.8 M Q^+ ($Q^+ = Li^+$, Na^+, Rb^+) and 1.8 M NO_3^- brought the fluorescence lifetime of uranyl down to approximately 1.5 μs. This slight decrease in the fluorescence lifetime could be explained by weak dynamic quenching facilitated by the addition of cations and/or the contributions of fluorescence from $UO_2^{2+}(NO_3^-)_n$ complexes. However, there is evidence that exponential regions

of the fluorescence decay were not significantly influenced by the formation of nitrate complexes. Fig. 1 of ref. 3 shows that fluorescence detection at 510 nm favors the bare UO_2^{2+} ion while detection at 500 nm favors the complexes. Fig. 2 (present work) shows time-resolved fluorescence traces for a 1.8 M solution of $NaNO_3$ recorded using detection of 510 and 500 nm light. Non-exponential kinetics were observed at short times, and the data for 510 nm detection have been shifted by 300 ns to superimpose the exponential decay regions. The inset in Fig. 2 shows the difference between the two fluorescence signals. From this plot it is apparent that the decay characteristics of the bare UO_2^{2+} ion and the nitrate complexes were closely similar.

As discussed below, many of the time-resolved fluorescence curves deviated from single exponential decay at the earliest times, but the longer-lived fluorescence was well represented by exponential decay. Fig. 3 shows a typical example, where the exponential decay portion of the curve corresponded to the fluorescence decay $(T_1(^3\Delta) \rightarrow S_0(^1\Sigma^+))$ of the bare and complexed uranyl species. The analyses of the quenching kinetics used the single exponential decay regions of the curves to determine the decay rates.

The quaternary ammonium cation's ability to quench uranyl fluorescence was also studied. While NH_4^+ and TEA^+ were found to be inefficient quenchers, the presence of TMA^+ significantly reduced the lifetime. Fig. 4 shows the fluorescence decay curves from solutions containing 1.8 M of $Q^+(NO_3)^-$ ($Q^+ = Li^+$, Na^+, Rb^+, TMA^+, TEA^+). The presence of 1.8 M TMA^+ in solution reduced the fluorescence lifetime to 580 ns, revealing TMA^+ to be a markedly more effective quencher. Similar to the results observed by Clark *et al.*,[7] smaller or larger ammonium cations were less effective quenching species (comparable to the alkali metal cations). These results indicate that TMA^+ is involved in a unique interaction with UO_2^{2+}. Hence, investigating how the presence of TMA^+ affects uranyl fluorescence decay under changing conditions such as temperature and concentration may provide new insights concerning the TMA^+
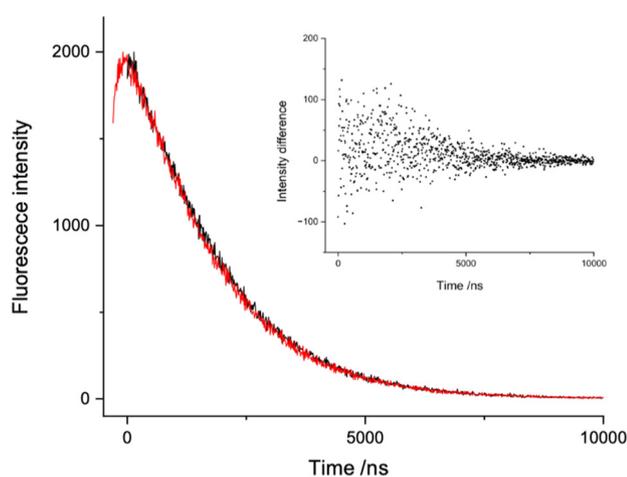

Fig. 2 Time-resolved fluorescence curves for UO_2^{2+} in 1.8 M $NaNO_3$ solution. The red and black curves correspond to fluorescence detection at 500 and 510 nm. The inset shows the difference between these curves.
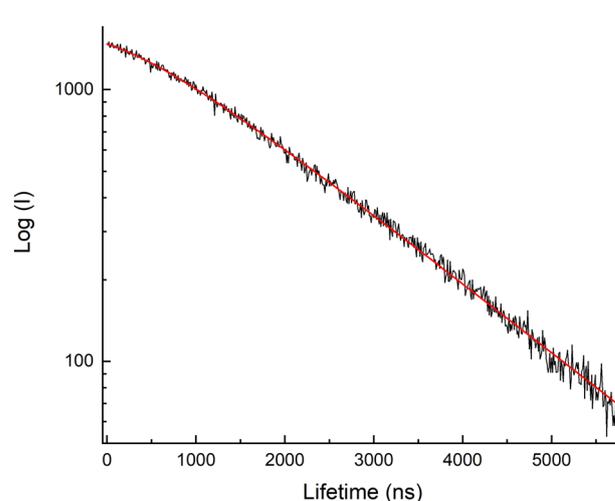

Fig. 3 Semi-log plot of the time-resolved fluorescence from a uranyl solution that contained 1.8 M $NaNO_3$ at 20 °C.

10168 | *Phys. Chem. Chem. Phys.*, 2025, **27**, 10166–10173

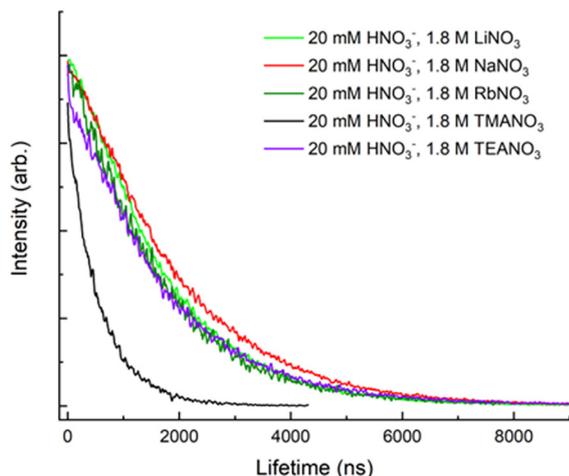This journal is © the Owner Societies 2025

Paper

Fig. 4 Fluorescence decay of uranyl at 510 nm, with an excitation wavelength of 394 nm and T = 20 °C. Each solution had a salt concentration of 1.8 M.

quenching mechanism and its ability to prevent hydroxide precipitation in alkaline solutions.

3.3. Temperature-dependant measurements

To explore the quenching effects of the cations thermodynamically, the temperature dependence of the decay rates was measured using solutions containing 1.8 M of quenching ions. Fig. 5a shows the decay rates of UO_2^{2+} fluorescence in H_2O and their dependence on temperature was consistent with the Arrhenius expression.[2,19] The expression in the form:

$$\ln(\Gamma) = \ln(A) - \frac{E_a}{RT} \qquad (3)$$

where Γ is the observed decay rate, A is a pre-exponential factor, E_a is the activation energy, R is the gas constant and T is the absolute temperature, yielded the $\ln(A)$ and E_a values listed in Table 1. The results show that the presence of TMA^+ had a

Table 1 Arrhenius fitting parameters for uranyl fluorescence decay rates. Cation concentrations were 1.8 M

Ion	ln(A)/H_2O	E_a/H_2O, kJ Mol^{-1}	ln(A)/D_2O	E_a/D_2O, kJ mol^{-1}
Li$^+$	27.6	34.3	28.1	36.3
Na$^+$	30.2	41.3	30.2	42.2
Rb$^+$	30.2	41.0		
NH$_4^+$	30.7	42.4		
TMA$^+$	24.9	25.8	24.3	24.8
d-TMA$^+$			24.6	25.9
TEA$^+$	26.2	31.0		

significant effect on the activation energy for the quenching of UO_2^{2+} fluorescence as compared to the other cations of this study. For the ions Na^+, Rb^+ and NH_4^+ the similarity of the decay rates and their temperature dependencies indicated that quenching by H_2O dominated the kinetics. The activation energies were consistent with the values obtained in previous studies of the quenching by H_2O^2. The activation energy associated with quenching UO_2^{2+} by TMA^+ was the lowest at E_a = 25.8 kJ mol^{-1}, indicating that quenching by TMA^+ was more accessible as compared to H_2O. Fig. 5b shows fluorescence decay rates recorded as a function of temperature in D_2O. Comparing Fig. 5a and b, it is evident that the decay rates were reduced by deuteration of the solvent, but in the case of TMA^+ the H_2O/D_2O decay rate ratio was much closer to 1:1. This would be expected if quenching by TMA^+ was dominant over the quenching by H_2O/D_2O.

3.4. Concentration-dependant measurements

The relationship between quencher concentration and uranyl fluorescence decay rate was used to investigate the quenching process between UO_2^{2+} and the cations. Experiments were carried out at a fixed temperature (20 °C) for quenching ion concentrations ranging from 0 to 1.8 M. Decay rate *versus* concentration data (referred to as Stern–Volmer plots in the following) were fitted using the expression:
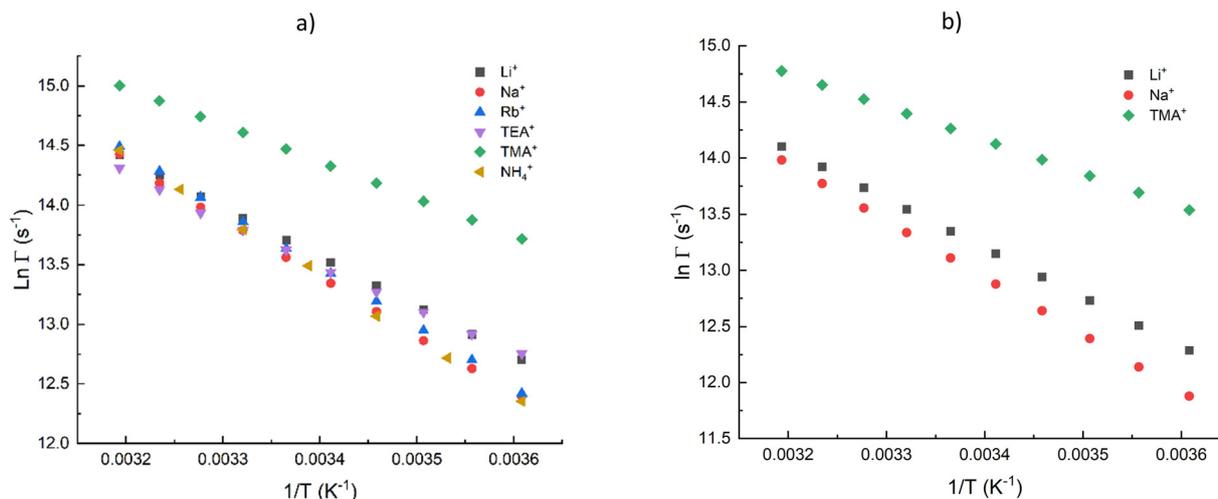

Fig. 5 Fluorescence decay rates as a function of temperature. (a) Measurements were carried out in H_2O with added nitrate salt concentrations of 1.8 M. (b) Measurements were carried out in D_2O with added nitrate salt concentrations of 1.8 M.

$$\Gamma = \Gamma_0 + k(Q^+)[Q^+] \qquad (4)$$

where $[Q^+]$ is the concentration of the quenching ion, Γ_0 is the $[Q^+] = 0$ decay rate and $k(Q^+)$ is the 20 °C quenching rate constant. To probe the $k(Q^+)$, all other ions in solution were held constant (20 mM $[H^+]$, 20 mM $[UO_2^{2+}]$, and 1.86 M $[NO_3^-]$). To maintain a constant $[NO_3^-]$, any decrease in $[Q^+]$ was matched by an increase in $[Na^+]$. Fig. 6 shows the Stern–Volmer plot for the $[Li^+]$ series, where a linear slope indicated that Li^+ participated in dynamic quenching of UO_2^{2+}.

The observable quenching rate constants measured in H_2O and D_2O are listed in Table 2. Due to the dominance of solvent quenching, we could not extract statistically significant quenching rate constants for Na^+, Rb^+ or NH_4^+. Quenching by Li^+ was fast enough for determination of the rate constant, and the Stern–Volmer plot for TEA^+ yielded a rate constant that was similar to that of Li^+ (cf. Table 2). Given that NH_4^+ and TEA^+ were found to be ineffective quenchers, it was surprising to discover that TMA^+ was the most effective quencher examined in this study. Again, we saw that deuteration of the solvent had a smaller effect on the quenching rate for TMA^+ as compared to the alkali metals. Li^+ appears to quench by a dynamic process that involves the solvent, while TMA^+ participates in quenching directly with UO_2^{2+}.

The Stern–Volmer (S–V) plots for TMA^+ and TEA^+ also indicated that quenching was not purely collisional as their data deviated from a straight line. Fig. 7 shows S–V plots for TMA^+ in H_2O and D_2O. The reason for this negative curvature is unclear, but we have assumed that the quenching rate constant can be defined by the linear coefficient of a quadratic fit to the S–V data. The rate constants determined using this method are listed in Table 2.

3.5. Non-exponential decay kinetics

The deviation from single exponential decay observed in solutions where the quenching was slow was another surprising detail of the decay kinetics. This effect was noted even for stock solutions that contained just 0.06 M nitrate, where the
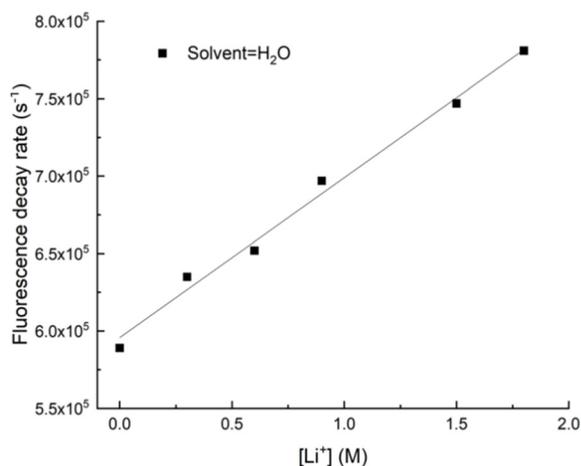
Table 2 Rate constants for quenching of uranyl fluorescence at 20 °C

Ion	$k(Q^+)/10^4$ dm³ mol⁻¹ s⁻¹ Solvent = H_2O	$k(Q^+)/10^4$ dm³ mol⁻¹ s⁻¹ Solvent = D_2O
Li^+	11.7	5.0
Na^+	a	
Rb^+	a	
NH_4^+	a	
TMA^+	100	111
TEA^+	10.6	

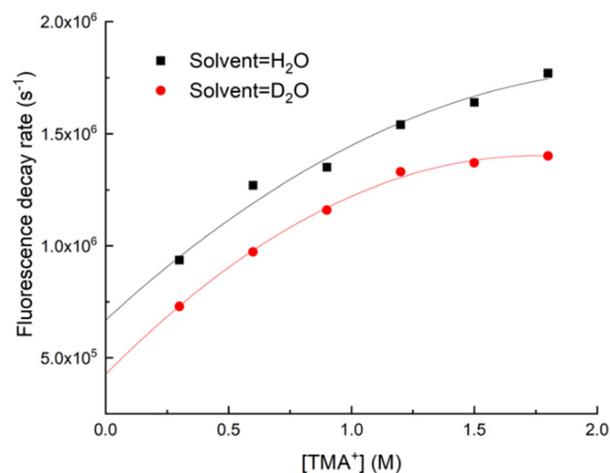[a] The quenching constant for the cation was not measurable.

Fig. 7 Decay rate vs. TMA^+ concentration for uranyl fluorescence from H_2O and D_2O solutions. Measurements taken at 20 °C.

concentration of uranyl nitrate complexes would have been insignificant.

Several steps were taken to ensure that the presence of a non-exponential decay component was not due to signal saturation of the PMT detector. When photon signals are counted using a MCS method, the dynamic range of fluorescence intensity for species with decay lifetimes <1 μs is low. To avoid saturation of the detector, emission intensities were kept low using neutral density filters. For additional verification, the fluorescence decay from a sample containing 20 mM $[UO_2^{2+}]$, 20 mM $[HNO_3]$ and 1.8 M $[NaNO_3]$ in H_2O was measured using an analogue detection method with a far greater dynamic range. The non-exponential decay was observed in this alternative detection method, reproducing the temporal behavior obtained using MCS detection.

It is well established that, following excitation at short wavelengths (e.g., $\lambda < 400$ nm), UO_2^{2+} undergoes rapid non-radiative relaxation to the emitting state.[15,16] Haubitz et al.[9] assigned the state of UO_2^{2+} excited by light near 310 nm to $T_2(^3\Phi_g)$ which relaxes to the $T_1(^3\Delta_g)$ emitting state. For water-coordinated UO_2^{2+} they reported a non-radiative rate for transfer from $T_2(^3\Phi_g)$ to $T_1(^3\Delta_g)$ of 3.5×10^{11} s⁻¹. Ghosh et al.[18] followed the ultra-fast relaxation kinetics for UO_2^{2+} in nitric acid solutions using 400 nm excitation. They proposed that the $^1\Phi_g$ state was initially excited, with relaxation down to the

Fig. 6 Decay rate vs. Li^+ concentration for uranyl fluorescence from H_2O solutions. Measurements taken at 20 °C.

emitting $^3\Delta_g$ state occurring on a picosecond timescale. The relaxation kinetics observed using ultrafast techniques occurred at rates that were too fast to be observed using the equipment available for the present study, and could not account for the observed deviations from single exponential decay.

We observed decay curves where there was a slower rate of decay at earlier times. This indicates that there is a minor, slow relaxation channel that feeds population to the emitting state. Consequently, the non-exponential decay curves have been simulated using the kinetic scheme shown in Fig. 8. We propose that there are overlapping electronic transitions excited at wavelengths near 394 nm. The dominant absorption populates excited states that are subject to rapid non-radiative relaxation. A weaker transition populates a state that has a lower rate of relaxation to the emitting state, resulting in a transfer that was slow enough to be observed. Fig. 8 shows an energy level scheme for this model, where state 3 represents excitation to $T_2(^3\Phi_g)$ (and other states that relax rapidly to $T_1(^3\Delta_g)$). Γ_{31} is the rapid relaxation channel which is fast enough that we can consider this to be direct excitation of state 1. State 2 is the state (or group of states) with the slow relaxation rate. For this situation the time dependence of the emission signal is given by:

$$I(t) =$$
$$N\left(f \cdot \mathrm{Exp}(-\Gamma_{10}t) + (1-f)\frac{\Gamma_{21}}{\Gamma_{21}-\Gamma_{10}}(\mathrm{Exp}(-\Gamma_{10}t) - \mathrm{Exp}(-\Gamma_{21}t))\right)$$
$$(5)$$

where N is a constant of proportionality, Γ_{10} is the decay rate from the emitting state ($\Gamma_{10} = \Gamma_0 + k(Q^+)[Q^+]$), Γ_{21} is the non-radiative relaxation rate for the slow channel, and f is the fractional contribution from excitation of state 3 to the emission signal. This can be influenced by the excitation and detection wavelengths. Fig. 3 shows a fit of eqn (5) to the data for a solution containing 1.8 M of $NaNO_3$ (excitation at 394 nm and detection at 510 nm). The parameters defined by this fit were $\Gamma_{10} = 5.9 \times 10^5$ s^{-1}, $\Gamma_{21} = 14.7 \times 10^5$ s^{-1}, and $f = 0.8$. Fitting of several other fluorescence decay curves recorded with
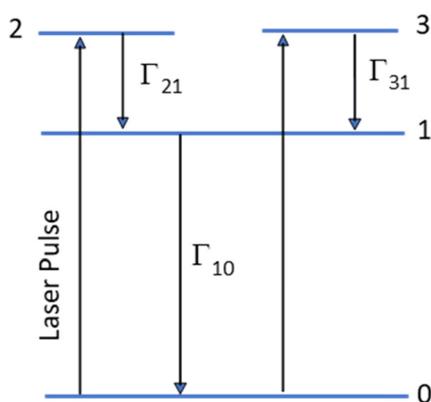

Fig. 8 Proposed energy level scheme for the non-exponential fluorescence decay of uranyl. See text for details.

$[NO_3^-] = 1.8$ M yielded a consistent set of f and Γ_{21} parameters ($0.76 \le f \le 0.82$; $1.4 \times 10^6 \le \Gamma_{21} \le 1.6 \times 10^6$ dm^3 mol^{-1} s^{-1}).

4. Discussion

There have been several previous studies of the quenching of UO_2^{2+} fluorescence in the presence of metal cations. Moriyasu et al.[20] noted that the alkali metal cations were closed-shell species that could not be expected to affect quenching by electron or energy transfer mechanisms. They reported that the ions Li$^+$, Na$^+$, K$^+$, Rb$^+$ and Cs$^+$ had quenching rate constants that were less than an upper bound of 10^4 dm^3 mol^{-1} s^{-1} at a temperature of 25 °C. The present results for Na$^+$ and Rb$^+$ are consistent with this observation, but the quenching rate constant for Li$^+$ was found to be an order of magnitude greater than the upper bound of Moriyasu et al.[20] Furthermore, it was possible to characterize the Li$^+$ quenching rate in D_2O, where the rate constant was approximately half the value measured in H_2O. The Li$^+$ measurements were repeated using several different LiNO$_3$ solutions to check for the presence of impurities. These experiments yielded consistent results and no evidence of contaminants. It is difficult to rationalize why Li$^+$ would be a more effective quencher than either Na$^+$ or Rb$^+$. This is clearly inconsistent with a heavy element effect. The marked decrease of the rate constant on switching from H_2O to D_2O indicates that the solvent is involved in the quenching mechanism. It is also of interest to note that the effective activation energy for quenching by Li$^+$ is lower than that for quenching by H_2O or D_2O alone.

Time-resolved fluorescence curves that deviated from single exponential decay were observed under conditions where the quenching rates were low. We speculate that this behavior is a consequence of the excitation of overlapping absorption bands. Quantitative analysis of the decay curves was achieved using a model where one of the initially excited states had a measurable rate for non-radiative relaxation into the emissive $T_1(^3\Delta)$ electronic state. There is no precedent for the slow relaxation rate needed for this kinetic model. We note, however, that many excited electronic states are accessible at an excitation energy of $25\,380$ cm^{-1} (394 nm). This is evident from the many published discussions of the electronic states of UO_2^{2+}, including the work of Denning,[17] Ghosh,[18] De Houwer and Gorller-Walrand,[21] and Haubitz and co-workers.[9] In a study of cryogenic matrix isolated UO_2Cl_2, Jin et al.[22] observed seven electronically excited states of UO_2^{2+} at energies in the range of 20 338 to 26 000 cm^{-1}. Decay channels with rates on the order of 1.5×10^6 s^{-1} were not observed as the fluorescence decay in the matrix was bi-exponential with lifetimes of 50(5) and 260(20) μs.

Quenching by the quaternary ammonium cations NH$_4^+$, TMA$^+$ and TEA$^+$ was also found to follow a non-monotonic dependence on the size of the cation. For these molecules, it might be expected that electronic to vibrational energy transfer would be an available deactivation mechanism. However, if this was a significant channel it would be probable that TEA$^+$, having the highest density of vibrational states, would be the

This journal is © the Owner Societies 2025

Phys. Chem. Chem. Phys., 2025, **27**, 10166–10173 | **10171**

most efficient quencher. Hydrogen abstraction is another possible quenching mechanism for the quaternary ammonium cations, but this is not supported by the available data. Comparing the fluorescence decay rates for TMA^+ and $d\text{-}TMA^+$ in D_2O, deuteration of TMA^+ had a weak effect on the fluorescence decay rate, reducing the value at 20 °C from 1.36×10^6 s^{-1} to 1.17×10^6 s^{-1} (1.8 M solutions). This 4% change does not seem to be consistent with H/D atom transfer.

Conclusions

We have analyzed the emission spectra and time-resolved fluorescence decay of UO_2^{2+} in nitric acid and studied the quenching ability of various nitrate salts $Q^+(NO_3)^-$ ($Q^+ = Li^+$, Na^+, Rb^+, NH_4^+, TMA^+, and TEA^+) on uranyl. The addition of 1.8 M NO_3^- resulted in the broadening of emission spectra associated with an increase in uranyl nitrate complexation and the extent of complexation was dependent on the cation of the nitrate salt. In agreement with previous studies, we found that quenching of uranyl fluorescence by Na^+ and Rb^+ is negligibly slow under low pH conditions. Quenching by Li^+ was found to be slow, but measurable in both H_2O and D_2O solutions. The solvent dependence of the Li^+ quenching rate constant at 20 °C suggests that an interaction between Li^+ and H_2O/D_2O is part of the dynamic quenching mechanism.

Quenching of uranyl by the quaternary ammonium cations was found to be insignificant for NH_4^+, slow for TEA^+ and relatively fast for TMA^+ (by an order of magnitude as compared to TEA^+). In this context, it is of interest to note that NH_4^+, TMA^+ and TEA^+ were previously investigated for their ability to inhibit the formation of insoluble uranyl hydroxide complexes under alkaline conditions. Clark et al.[7] concluded that, "We have shown that monomeric uranyl hydroxides, $UO_2(OH)_4^{2-}$ and $UO_2(OH)_5^{3-}$, can be stabilized from uranate formation using the Me_4N^+ (TMA^+) cation, thereby allowing for a full characterization under highly alkaline conditions. TMA^+ seems to be unique in this regard, as larger or smaller ammonium ions were unsuccessful at preventing precipitation." Hence, it appears that there may be a link between the quenching behavior and the selective inhibition of uranyl precipitation in the presence of TMA^+.

Author contributions

Thomas D. Persinger: conceptualization, investigation, formal analysis, visualization, and writing – original draft and review & editing. Michael C. Heaven: investigation, formal analysis, and writing – review and editing. Richard E. Wilson: conceptualization, funding acquisition, supervision and writing – review & editing.

Data availability

The data supporting this article have been included as part of the ESI.†

Conflicts of interest

There are no conflicts to declare.

Acknowledgements

Notes and references

1 *Ion exchange and solvent extraction: a series of advances*, ed. B. A. Moyer, 2010, vol. 19.

2 M. D. Marcantonatos, Photochemistry and exciplex of the uranyl ion in aqueous solution, *J. Chem. Soc., Faraday Trans. 1*, 1980, **76**(5), 1093–1115.

3 C. Moulin, P. Decambox, P. Mauchien, D. Pouyat and L. Couston, Direct Uranium(VI) and Nitrate Determinations in Nuclear Reprocessing by Time-Resolved Laser-Induced Fluorescence, *Anal. Chem.*, 1996, **68**(18), 3204–3209.

4 A. B. Yusov and V. P. Shilov, Reduction of the photoexcited uranyl ion by water 1. U(IV) and H_2O_2 formation, *Russ. Chem. Bull.*, 2000, **49**(2), 285–290.

5 T. Haubitz, B. Drobot, S. Tsushima, R. Steudtner, T. Stumpf and M. U. Kumke, Quenching Mechanism of Uranyl(VI) by Chloride and Bromide in Aqueous and Non-Aqueous Solutions, *J. Phys. Chem. A*, 2021, **125**(20), 4380–4389.

6 D. A. Palmer and C. Nguyen-Trung, Aqueous uranyl complexes. 3. Potentiometric measurements of the hydrolysis of uranyl(VI) ion at 25 °C, *J. Solution Chem.*, 1995, **24**(12), 1281–1291.

7 D. L. Clark, S. D. Conradson, R. J. Donohoe, D. W. Keogh, D. E. Morris, P. D. Palmer, R. D. Rogers and C. D. Tait, Chemical Speciation of the Uranyl Ion under Highly Alkaline Conditions. Synthesis, Structures, and Oxo Ligand Exchange Dynamics, *Inorg. Chem.*, 1999, **38**(7), 1456–1466.

8 M. D. Marcantonatos and M. Deschaux, Electron transfer and aqua cation-cation complex formation in the excited state of the uranyl ion, *Chem. Phys. Lett.*, 1980, **76**(2), 359–365.

9 T. Haubitz, S. Tsushima, R. Steudtner, B. Drobot, G. Geipel, T. Stumpf and M. U. Kumke, Ultrafast Transient Absorption Spectroscopy of UO_2^{2+} and $[UO_2Cl]^+$, *J. Phys. Chem. A*, 2018, **122**(35), 6970–6977.

10 H. D. Burrows and S. J. Formosinho, Photochemical hydrogen abstractions as radiationless transitions. Part 3. Theoretical analysis of hydrogen abstraction by excited uranyl (UO_2^{2+}) ion, *J. Chem. Soc., Faraday Trans. 2*, 1977, **73**(2), 201–208.

11 S. J. Formosinho, H. D. Burrows, M. da Graca Miguel, M. E. D. G. Azenha, I. M. Saraiva, A. C. D. N. Ribeiro,

10172 | *Phys. Chem. Chem. Phys.*, 2025, **27**, 10166–10173

This journal is © the Owner Societies 2025

I. V. Khudyakov, R. G. Gasanov, M. Bolte and M. Sarakha, Deactivation processes of the lowest excited state of $[UO_2(H_2O)_5]^{2+}$ in aqueous solution, *Photochem. Photobiol. Sci.*, 2003, **2**(5), 569–575.

12 M. D. Marcantonatos, Dual luminescence of uranyl and self-quenching in aqueous acidic solution, *Inorg. Chim. Acta*, 1978, **26**(1), 41–46.

13 M. D. Marcantonatos, The exciplex formation between uranyl species further evidenced by quenching data of the UO_2^{2+} luminescence, *Inorg. Chim. Acta*, 1977, **24**(2), L37–L39.

14 R. Nagaishi, T. Kimura, J. Inagawa and Y. Kato, Isotope and temperature effects on photochemical reactions of uranyl ion in H_2O-D_2O mixtures, *J. Alloys Compd.*, 1998, **271–273**, 794–798.

15 C. P. Baird and T. J. Kemp, Luminescence, spectroscopy, lifetimes and quenching mechanisms of excited states of uranyl and other actinide ions, *Prog. React. Kinet.*, 1997, **22**(2), 87–139.

16 H. D. Burrows and T. J. Kemp, Photochemistry of the uranyl ion, *Chem. Soc. Rev.*, 1974, **3**(2), 139–165.

17 R. G. Denning, Electronic Structure and Bonding in Actinyl Ions and their Analogs, *J. Phys. Chem. A*, 2007, **111**(20), 4125–4143.

18 R. Ghosh, J. A. Mondal, H. N. Ghosh and D. K. Palit, Ultrafast Dynamics of the Excited States of the Uranyl Ion in Solutions, *J. Phys. Chem. A*, 2010, **114**(16), 5263–5270.

19 M. Moriyasu, Y. Yokoyama and S. Ikeda, Quenching of uranyl luminescence by water molecule, *J. Inorg. Nucl. Chem.*, 1977, **39**(12), 2211–2214.

20 M. Moriyasu, Y. Yokoyama and S. Ikeda, Quenching mechanisms of uranyl luminescence by metal ions, *J. Inorg. Nucl. Chem.*, 1977, **39**(12), 2205–2209.

21 S. De Houwer and C. Gorller-Walrand, Influence of complex formation on the electronic structure of uranyl, *J. Alloys Compd.*, 2001, **323–324**, 683–687.

22 J. Jin, R. Gondalia and M. C. Heaven, Electronic Spectroscopy of UO_2Cl_2 Isolated in Solid Ar, *J. Phys. Chem.*, 2009, **113**, 12734–12738.

This journal is © the Owner Societies 2025

Phys. Chem. Chem. Phys., 2025, **27**, 10166–10173 | 10173